



ProMISe: Promptable Medical Image Segmentation using SAM

Jinfeng Wang^{1,2,4*}, Sifan Song^{3*}, Xinkun Wang^{1*}, Yiyi Wang^{1*}, Yiyi Miao^{1,2},
Jionglong Su¹ , and S. Kevin Zhou^{4,5} 

¹ School of AIAC, Xi'an Jiaotong-liverpool University, Suzhou, China

² University of Liverpool, Liverpool, UK

³ Center of Advanced Medical Computing and Analysis, Massachusetts General Hospital and Harvard Medical School, Boston, MA 02114, USA

⁴ School of BME & Suzhou Institute for Advanced Research, Center for Medical Imaging, Robotics, Analytic Computing & Learning (MIRACLE), University of Science and Technology of China, Suzhou, China

⁵ Key Lab of Intelligent Information Processing of Chinese Academy of Sciences, Institute of Computing Technology, CAS, Beijing, China

Jionglong.Su@xjtlu.edu.cn

s.kevin.zhou@gmail.com

Abstract. With the proposal of the Segment Anything Model (SAM), fine-tuning SAM for medical image segmentation (MIS) has become popular. However, due to the large size of the SAM model and the significant domain gap between natural and medical images, fine-tuning-based strategies are costly with potential risk of instability, feature damage and catastrophic forgetting. Furthermore, some methods of transferring SAM to a domain-specific MIS through fine-tuning strategies disable the model's prompting capability, severely limiting its utilization scenarios. In this paper, we propose an Auto-Prompting Module (APM), which provides SAM-based foundation model with Euclidean adaptive prompts in the target domain. Our experiments demonstrate that such adaptive prompts significantly improve SAM's non-fine-tuned performance in MIS. In addition, we propose a novel non-invasive method called Incremental Pattern Shifting (IPS) to adapt SAM to specific medical domains. Experimental results show that the IPS enables SAM to achieve state-of-the-art or competitive performance in MIS without the need for fine-tuning. By coupling these two methods, we propose **ProMISe**, an end-to-end non-fine-tuned framework for **Promptable Medical Image Segmentation**. Our experiments demonstrate that both using our methods individually or in combination achieves satisfactory performance in low-cost pattern shifting, with all of SAM's parameters frozen.

Keywords: SAM · Medical image segmentation · Pattern shifting

 The corresponding authors

* These authors contributed equally to this work

The code can be found at <https://github.com/xinkunwang111/ProMISe>

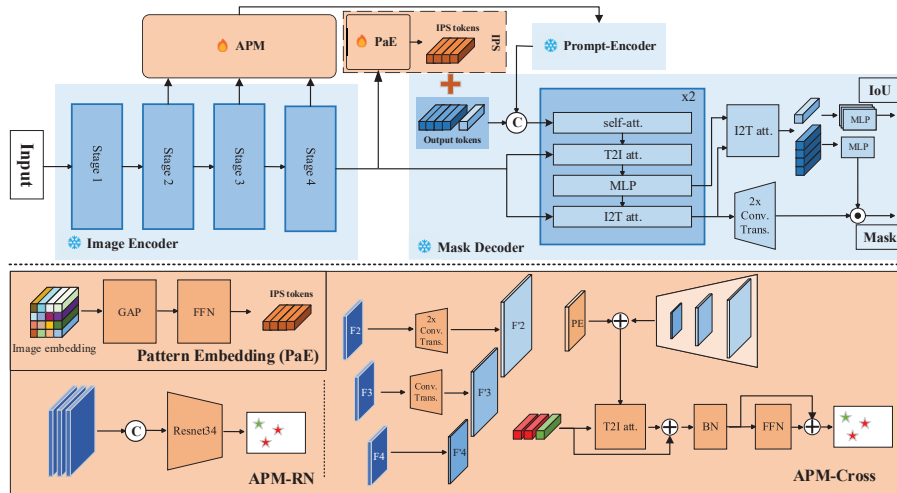


Fig. 1. Overview of PromISE. All three components of the original SAM are frozen. The **Auto-Prompting Module (APM)** leverages features from the image encoder to predict optimal prompts in Euclidean space. The APM can be implemented using various operators and modules, such as CNN and Transformer. The **Pattern Embedding (PaE)** module analyzes the image embedding to extract pattern gaps between the target and source domains. The **Incremental Pattern Shifting (IPS)** tokens are added to the mask tokens of the output tokens to realize the decoder’s shifting of mask patterns.

1 Introduction

Recently, many large-scale foundation models [2,27] deliver exciting performance with promising results in various domains. Among them, the latest one SAM [2], a foundation model for natural image segmentation, has attracted significant attention from researchers in the computer vision community. SAM enables interactive segmentation of targets through prompts such as points, bounding boxes, masks, and text. Medical Image Segmentation (MIS) tasks are crucial in medical image analysis. Unlike natural images, medical images contain diverse and distinctive data modalities and application scenarios. The transfer and deployment of SAM for MIS present a meaningful and promising research area.

Some studies [10,11,12,13] have explored the capability of SAM in MIS in a zero-shot fashion. Unfortunately, their results demonstrate that neither points or bounding boxes guided by ground truth (GT), nor the automated methods of SAM, can achieve satisfactory and practical performance in MIS. Also, different studies have used various prompts (such as latent representations [1,3], bounding boxes [4,5,6], text [6,7], mask [5], points [5,6]) by different strategies (*e.g.*, all-parameter fine-tuning [4], adapter [6,8], bias-tuning [7], and LoRA [3]) to different degrees (decoder-only [9], prompt-encoder-only [1], and all components

[4]), with the aim of fine-tuning SAM for transfer to the target domain. However, since SAM is a large foundation model trained on extensive datasets, these fine-tuning-based approaches incur enormous training costs and face potential risks of instability, feature damage and catastrophic forgetting. Such fine-tuning-based transfer methods typically utilize the model as a heavy pre-trained model rather than a foundation model.

In this paper, we rethink the use of each component of SAM in the following way. First, the prompt encoder, as a mapping between Euclidean and latent space, has been adequately trained during the training process of SAM. Some studies attempt to use latent representations instead of explicit Euclidean prompts to automate the SAM model, but this approach sacrifices its interactive capability and interpretability. Second, as a foundation model trained on extensive datasets with a complex training strategy, the encoder of SAM already possesses robust feature extraction capabilities. We argue that utilizing these capabilities efficiently and properly in unseen domains is more valuable than fine-tuning them. Third, by analyzing the mask decoder, we observe that the output tokens provide prior pattern knowledge for mask prediction based on prompts. Therefore, we claim that pattern shifting of output tokens can achieve more efficient and stable domain adaptation for SAM compared to fine-tuning.

As demonstrated in Fig. 1, based on the above arguments: 1) We propose the Auto-Prompting Module (APM), which leverages the SAM framework for training and provides adaptive Euclidean prompts for SAM; 2) We propose Incremental Pattern Shifting (IPS), a novel non-invasive pattern shifting method which couples a Pattern Embedding (PaE) module with IPS tokens to cost-effectively shift the prior pattern knowledge of the mask decoder. The IPS method enables SAM to achieve state-of-the-art (SOTA) and competitive performance without the need for fine-tuning; 3) We couple the above two methods to propose the **Promptable Medical Image Segmentation (ProMISe)** framework utilizing SAM. Notably, we are the first to propose methods for transferring SAM to MIS while keeping **all of SAM’s parameters frozen**, resulting in significantly reduced training costs, improved stability, and the ability to retain spatial prompting capability.

2 Method

2.1 Adaptive Prompt

Several zero-shot studies [10,11,12,13] utilize the interactive capability of SAM to investigate its potential as a large-scale foundation model for transferring to MIS tasks in an untrained manner. However, most of these approaches employ GT-based prompts, which are generated from GT masks using various different methods, such as GT-based foreground-background point sampling and noisy GT-bounding box. However, these GT-based prompt strategies fail to enable SAM to achieve practical performance in MIS tasks. We argue that this limitation is due to the coupling of prompts, image embeddings and mask patterns. In other words, without effectively utilizing image embeddings and transferring

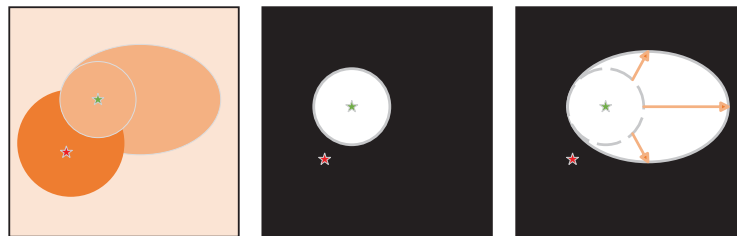


Fig. 2. Theoretical illustration of IPS. Left: Image with point prompts; Middle: Output mask from vanilla SAM; Right: Output mask from SAM with IPS. Arrows represent patterns shifting.

mask patterns, it remains challenging for SAM to consistently deliver satisfactory performance in unseen domains by only relying on GT-based spatial prompts.

As shown in Fig. 1, we design a lightweight end-to-end module, called Auto-Prompting Module (APM), which effectively integrates the multi-level features of SAM’s image encoder to predict optimal prompts in Euclidean space. By generating adaptive prompts that provide more fine-grained spatial information, the APM significantly enhances the untrained performance of SAM in the target domain. This indicates the highly expressive feature extraction capability of SAM, even in previously unseen domains.

During our research, we notice a significant performance limitation when using bounding boxes as prompts. We attribute this to the fact that bounding boxes only provide coarse-grained location information and lack fine-grained details. Thus, we mainly utilize point-based prompts in this paper. It is worth noting that our method is applicable to any form of prompts except text, and the APM can be implemented using various operators and modules (*e.g.*, ResNet34 and a simple cross-attention block).

2.2 Incremental Pattern Shifting (IPS)

As mentioned above, many studies based on fine-tuning strategies have been proposed to improve the performance of SAM in MIS tasks. However, inappropriate fine-tuning is likely to weaken the original parameter distribution of SAM. As such, it becomes difficult to sufficiently adjust to the optimal target distribution, especially in medical datasets with distinctive domains, making fine-tuning SAM unstable and inefficient. From a broader perspective, a simple fine-tuning strategy for pattern shifting is regarded as the model as a heavily pre-trained model rather than a foundation model, resulting in degraded model capabilities.

After rethinking the components of the SAM, we observe that the SAM has a very efficient mask decoder that refers to DETR [14] and MaskFormer [15]. In this study, we find that in the mask decoder, output tokens initially receive the location information of the point of interest (PoI) or region of interest (RoI) from

the prompt encoder through self-attention. Subsequently, as shown in Fig. 1, output tokens extract semantic information from the image embedding through cross-attention, forming semantic patterns. Based on these findings, we argue that with a large amount of training, the output tokens can be regarded as the *pattern information* acquired from the source domain, enabling SAM to generate predicted masks based on PoI or RoI. Therefore, assuming the image encoder of SAM is sufficiently powerful and well-trained, transferring SAM to MIS can be equivalent to transferring the mask prediction patterns of SAM to MIS.

$$[IoU, Mask] = \text{MaskDecoder}(ImageEmbedding, T_{Pattern}, T_{Prompts}) \quad (1)$$

$$T_{Pattern} = \text{Concat}(T_{IoU}, (T_{Mask} + T_{IPS})) \quad (2)$$

$$T_{IPS} = \text{FFN}(\text{GAP}(ImageEmbedding)) \quad (3)$$

With the above arguments, we propose a method called Incremental Pattern Shifting (IPS). As shown in Fig. 1, we extract the *pattern shifting information* (IPS tokens) from the image embedding using a lightweight PaE module, and then non-invasively shift the patterns of the mask decoder by adding the IPS tokens to the mask tokens (Eqs. 1-3). In Fig. 2, the mask decoder, when provided with the same PoI, generates mask predictions that are more compatible with the target domain after pattern shifting. Notably, our experiments show the effectiveness of IPS, utilizing GT-based prompts for both training and inference, in enabling SAM to achieve SOTA or competitive performance in MIS tasks.

2.3 ProMISe framework

Our proposed IPS method effectively facilitates segmentation pattern shifting. However, using GT-based prompts for pattern transfer does not allow end-to-end training. In addition, GT-based prompt sampling introduces significant randomness, thereby posing challenges to the stability of the training process. Therefore, we couple the IPS method with APM to achieve end-to-end pattern shifting for SAM to target medical domains. Moreover, favored by the preservation of Euclidean spatial form prompts, the ProMISe framework can handle both automatic and manual prompts during inference while retaining its interpretability.

3 Experiments

3.1 Experimental Setup

We individually conduct experiments in two modalities: endoscopy and dermatoscopy. For endoscopy experiments, we follow the experimental setups of PraNet [16], DuAT [24], and SSFormer [17]. We extract 1450 images from Kvasir [18] and CVC-ClinicDB [21] as the training set. Tests are then conducted on EndoScene [22], Kvasir, CVC-ColonDB [19], and ETIS [23], using Mean Absolute Error (MAE), mean Dice, and mean IoU as metrics. For dermatoscopy, we use

ISIC2018 for training and testing, with mean Dice and mean IoU as metrics. We utilize ViT-B as the image encoder for all SAM-related methods in the experiments. In addition, we apply three prompt settings in training and inference, namely 3/5/16 points (1/2/8 positive + 2/3/8 negative, 3/5/16P, respectively).

We implement our methods in pytorch, using one TESLA A100 GPU. Adam optimizer and a learning rate of 0.00001 are employed. The training period is 200 epochs. Our loss is a combination of Dice and BCE loss.

Table 1. Quantitative comparison of the performance enhancement brought to SAM by adaptive prompts provided by APMs (RN and Cross). ^a Trainable Parameters.

Benchmarks		Kvasir			EndoScene			ColonDB		
Methods	TP ^a	mDice	mIoU	MAE↓	mDice	mIoU	MAE↓	mDice	mIoU	MAE↓
U-Net [28]	-	0.818	0.746	0.055	0.710	0.627	0.022	0.512	0.444	0.061
ResUNet++ [30]	-	0.821	0.743	0.048	0.707	0.624	0.018	0.483	0.410	0.064
SAM-5P	-	0.750	0.645	0.104	0.656	0.582	0.139	0.569	0.482	0.215
SAM-16P	-	0.719	0.620	0.140	0.692	0.613	0.118	0.548	0.467	0.228
APM-RN-5P	21.7M	0.741	0.645	0.060	0.781	0.689	0.016	0.594	0.501	0.056
APM-RN-16P	21.7M	0.797	0.706	0.046	0.789	0.694	0.013	0.595	0.502	0.051
APM-Cross-5P	44.3M	0.749	0.648	0.074	0.711	0.619	0.059	0.511	0.433	0.165
APM-Cross-16P	44.3M	0.789	0.697	0.051	0.794	0.699	0.018	0.616	0.517	0.059

3.2 Adaptive Prompt

As described in Sect. 2.1, to study the actual performance of vanilla SAM in MIS, we train and test two types of APMs, *i.e.*, ResNet34 (RN) and a one-layer cross-attention Transformer module (Cross), on polyp benchmarks. As shown in Tab. 1, the adaptive prompts generated by both APMs effectively improve the performance of SAM in the polyp segmentation task, achieving a level comparable to the baseline MIS segmentation model. Furthermore, we observe a significant reduction in MAE by increasing the number of point prompts with more provided fine-grained information, which suggests that our method effectively utilizes the boundary sensitivity of vanilla SAM.

3.3 Pattern Shifting

In Tab. 2, we train the proposed IPS method (PaE with 4 IPS tokens) using GT-based prompt points. We perform tests using the same GT-based point prompts for SAM-related models and compare our method (SAM with IPS) to SOTA methods, SAM and SAM-Med2D. As shown in Tab. 2, our proposed IPS significantly improves the performance of SAM on benchmarks, achieving mDice improvements of 10%-25% in Kvasir, 19%-31% in EndoScene, 25%-33% in ColonDB, 25%-32% in ETIS, and 18%-37% in ISIC2018. Compared to SAM-Med2D, which is trained on a large-scale medical dataset and utilizes a complex

Table 2. Quantitative comparison of our IPS, SOTA methods, and other SAM-based methods. Best-in-class results are bolded, while second-best results are underlined. The 3P|5P and 3P|16P represent training our IPS on 3 GT-based prompt points and testing them with 5 and 16 ones. ^a Number of Trainable Parameters. ^b Number of Endoscopy/Dermoscopy images is utilized in the corresponding training set. * Some test set images from the corresponding dataset may be seen in the training process.

Benchmarks			Kvasir		EndoScene		ColonDB		ETIS		ISIC2018	
Methods	TP ^a	Images ^b	mDice	mIoU	mDice	mIoU	mDice	mIoU	mDice	mIoU	mDice	mIoU
SOTA Methods												
U-net [28]	-	1450/2594	0.818	0.746	0.710	0.627	0.512	0.444	0.398	0.335	0.855	0.785
PraNet [16]	-	1450/2594	0.898	0.840	0.851	0.797	0.712	0.640	0.628	0.567	0.875	0.787
TransUNet [29]	-	1450/2594	<u>0.913</u>	<u>0.857</u>	0.893	0.660	0.781	0.699	<u>0.731</u>	<u>0.624</u>	<u>0.880</u>	<u>0.809</u>
SSFormer [17]	-	1450/2594	0.926	0.874	0.887	0.821	0.772	0.697	0.767	0.698	0.919	0.861
SAM-based Methods												
SAM-3P [2]	-	-	0.589	0.471	0.513	0.414	0.447	0.356	0.464	0.381	0.489	0.367
SAM-5P	-	-	0.750	0.645	0.656	0.582	0.569	0.482	0.541	0.472	0.687	0.569
SAM-16P	-	-	0.719	0.620	0.692	0.613	0.548	0.467	0.524	0.455	0.738	0.624
Med2D-3P [5]	184.5M	5838/7935	*0.821	*0.735	0.697	0.597	0.689	0.588	0.633	0.524	*0.872	*0.803
Med2D-5P	184.5M	5838/7935	*0.822	*0.735	0.722	0.623	0.686	0.576	0.677	0.571	*0.884	*0.813
Med2D-16P	184.5M	5838/7935	*0.832	*0.748	0.727	0.620	0.685	0.575	0.622	0.514	*0.893	*0.823
IPS-3P	1.3M	1450/2594	0.841	0.752	0.824	0.735	0.749	0.645	0.715	0.619	0.860	0.769
IPS-3P 5P	1.3M	1450/2594	0.843	0.750	0.844	0.752	0.793	0.689	0.798	0.700	0.868	0.778
IPS-3P 16P	1.3M	1450/2594	0.861	0.774	0.836	0.743	0.802	0.697	0.786	0.689	0.868	0.779
IPS-5P	1.3M	1450/2594	<u>0.855</u>	<u>0.772</u>	<u>0.854</u>	<u>0.764</u>	<u>0.819</u>	<u>0.716</u>	<u>0.801</u>	<u>0.704</u>	0.889	0.808
IPS-16P	1.3M	1450/2594	0.911	0.851	0.897	0.821	0.874	0.789	0.840	0.750	0.921	0.850

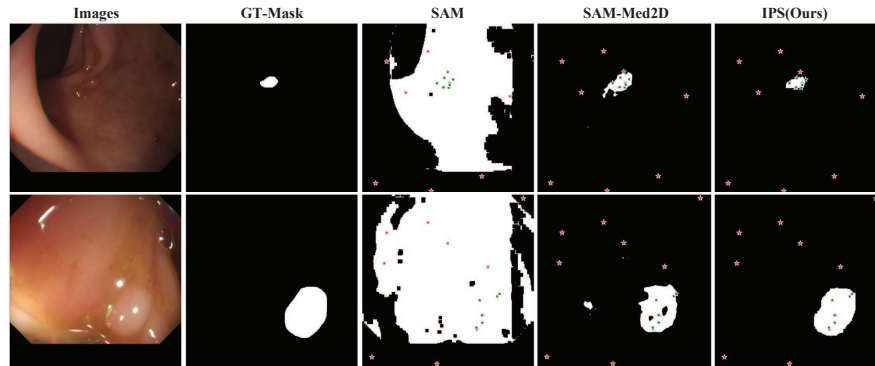


Fig. 3. Qualitative comparison of the performance with same prompts in ColonDB.

training strategy, our method also achieves a remarkable improvement. Experimental results indicate that the IPS method adequately leverages SAM’s powerful generalization and feature expression capabilities. Even in the unfamiliar and challenging benchmarks of ColonDB and ETIS, IPS enables SAM to achieve SOTA performance. Using SSFormer as a baseline, we obtain up to 10% and 7% improvement in ColonDB and ETIS, respectively. It is promising that the above performance improvement depends only on a tiny number of trainable parameters (1.3M), demonstrating that our IPS method is very lightweight and efficient.

Table 3. Performance of SAM with ProMISe (Cross and RN) is tested using GT-base prompts. ^a Number of Trainable Parameters. ^b Number of Endoscopy/Dermoscopy images is utilized in the corresponding training set. * Some test set images from the corresponding dataset may be seen in the training process.

Benchmarks			Kvasir		EndoScene		ColonDB		ETIS		ISIC2018	
Methods	TP ^a	Images ^b	mDice	mIoU	mDice	mIoU	mDice	mIoU	mDice	mIoU	mDice	mIoU
U-Net	-	1450/2594	0.818	0.746	0.710	0.627	0.512	0.444	0.398	0.335	0.855	0.785
ResUNet++	-	1450/2594	0.821	0.743	0.707	0.624	0.483	0.410	0.401	0.344	0.809	0.729
SAM-5P	-	-	0.750	0.645	0.656	0.582	0.569	0.482	0.541	0.472	0.687	0.569
SAM-16P	-	-	0.719	0.620	0.692	0.613	0.548	0.467	0.524	0.455	0.738	0.624
Med2D-5P	184.5M	5838/7935	*0.822	*0.735	0.722	0.623	0.686	0.576	0.677	0.571	*0.884	*0.813
Med2D-16P	184.5M	5838/7935	*0.832	*0.748	0.727	0.620	0.685	0.575	0.622	0.514	*0.893	*0.823
Cross-5P	45.6M	1450/2594	0.834	0.744	0.788	0.687	0.744	0.636	0.678	0.578	0.742	0.631
Cross-16P	45.6M	1450/2594	0.858	0.777	0.768	0.661	0.732	0.626	0.691	0.591	0.819	0.705
RN-5P	23.0M	1450/2594	0.776	0.673	0.705	0.587	0.664	0.547	0.605	0.508	0.798	0.688
RN-16P	23.0M	1450/2594	0.846	0.759	0.803	0.735	0.735	0.624	0.673	0.566	0.878	0.791

As demonstrated in Fig. 3 and Tab. 2, SAM and SAM-Med2D struggle to handle exposures and insignificant small-volume targets well, even when provided with more fine-grained guidance through an increased number of prompt points. In contrast, SAM with IPS significantly optimizes its predicted masks through non-invasive pattern shifting based on the same prompts (Fig. 3).

3.4 ProMISe framework

To avoid random sampling of prompts and thus achieve end-to-end pattern shifting, we propose the ProMISe framework, which couples the APM and IPS for training with adaptive prompts. When tested using GT-based prompts, the end-to-end pattern shifting of ProMISe with both APMs (Cross and RN) significantly improves SAM’s performance to a practical and competitive level in MIS (Tab. 3). Importantly, ProMISe maintains its interpretability using both adaptive/GT-based Euclidean prompts and keeps all of SAM’s parameters frozen, resulting in a more practical and applicable approach for real clinical scenarios.

3.5 Ablation Study

The IPS tokens significantly improve the performance, and the PaE module is indispensable for the IPS method to achieve SOTA results (Tab. 4). Using IPS tokens alone represents initialization of the tokens rather than being generated from the PaE. Thus, removing the PaE provides an extremely lightweight option.

4 Conclusions

In this paper, we propose a novel adaptive prompt generation module, Auto-Prompting Module (APM), which improves the non-fine-tuned performance of

Table 4. Ablation study for pattern shifting with 16 points (mDice scores). Mask tokens refer to unfreezing the mask tokens in SAM’s mask decoder. The optimal setting is in bold. ^a Number of Trainable Parameters.

Mask tokens	IPS tokens	PaE	Frozen SAM	TP ^a	Kvasir	EndoScene	ColonDB	ETIS
✓			✗	1.02K	0.581	0.796	0.756	0.726
	✓		✓	1.02K	0.862	0.817	0.802	0.778
	✓	✓	✓	1.29M	0.911	0.897	0.874	0.840

SAM in the target domain by generating optimal Euclidean prompts. In addition, we propose Incremental Pattern Shifting (IPS), which enables non-fine-tuned pattern shifting to improve SAM’s performance in unfamiliar domains, achieving SOTA and competitive results. Furthermore, we couple IPS with APM to propose the ProMISe framework, which realizes end-to-end pattern shifting. Benefiting from IPS, increasing prompt point number results in significant performance gains for SAM, which may be further extended to include scrawl, sketch or coarse prompts. More importantly, our results prove that a fine-tuning-based approach is not necessarily optimal for utilizing a foundation model like SAM.

Acknowledgments. This work was supported by Natural Science Foundation of China under Grant 62271465 and Open Fund Project of Guangdong Academy of Medical Sciences, China (No. YKY-KF202206).

References

1. T. Shaharabany, A. Dahan, R. Giryas, and L. Wolf, “Autosam: Adapting sam to medical images by overloading the prompt encoder,” *arXiv preprint arXiv:2306.06370*, 2023.
2. A. Kirillov, E. Mintun, N. Ravi, H. Mao, C. Rolland, L. Gustafson, T. Xiao, S. Whitehead, A. C. Berg, W.-Y. Lo *et al.*, “Segment anything,” *arXiv preprint arXiv:2304.02643*, 2023.
3. K. Zhang and D. Liu, “Customized segment anything model for medical image segmentation,” *arXiv preprint arXiv:2304.13785*, 2023.
4. Y. Li, M. Hu, and X. Yang, “Polyp-sam: Transfer sam for polyp segmentation,” *arXiv preprint arXiv:2305.00293*, 2023.
5. J. Cheng, J. Ye, Z. Deng, J. Chen, T. Li, H. Wang, Y. Su, Z. Huang, J. Chen, L. Jiang *et al.*, “Sam-med2d,” *arXiv preprint arXiv:2308.16184*, 2023.
6. J. Wu, R. Fu, H. Fang, Y. Liu, Z. Wang, Y. Xu, Y. Jin, and T. Arbel, “Medical sam adapter: Adapting segment anything model for medical image segmentation,” *arXiv preprint arXiv:2304.12620*, 2023.
7. J. N. Paranjape, N. G. Nair, S. Sikder, S. S. Vedula, and V. M. Patel, “Adaptivesam: Towards efficient tuning of sam for surgical scene segmentation,” *arXiv preprint arXiv:2308.03726*, 2023.
8. T. Chen, L. Zhu, C. Ding, R. Cao, S. Zhang, Y. Wang, Z. Li, L. Sun, P. Mao, and Y. Zang, “Sam fails to segment anything?—sam-adapter: Adapting sam in underperformed scenes: Camouflage, shadow, and more,” *arXiv preprint arXiv:2304.09148*, 2023.

9. J. Ma, Y. He, F. Li, L. Han, C. You, and B. Wang, "Segment anything in medical images," *Nature Communications*, vol. 15, no. 1, p. 654, 2024.
10. D. Cheng, Z. Qin, Z. Jiang, S. Zhang, Q. Lao, and K. Li, "Sam on medical images: A comprehensive study on three prompt modes," *arXiv preprint arXiv:2305.00035*, 2023.
11. T. Zhou, Y. Zhang, Y. Zhou, Y. Wu, and C. Gong, "Can sam segment polyps?" *arXiv preprint arXiv:2304.07583*, 2023.
12. M. A. Mazurowski, H. Dong, H. Gu, J. Yang, N. Konz, and Y. Zhang, "Segment anything model for medical image analysis: an experimental study," *Medical Image Analysis*, vol. 89, p. 102918, 2023.
13. S. He, R. Bao, J. Li, P. E. Grant, and Y. Ou, "Accuracy of segment-anything model (sam) in medical image segmentation tasks," *arXiv preprint arXiv:2304.09324*, 2023.
14. N. Carion, F. Massa, G. Synnaeve, N. Usunier, A. Kirillov, and S. Zagoruyko, "End-to-end object detection with transformers," in *European conference on computer vision*. Springer, 2020, pp. 213–229.
15. B. Cheng, A. Schwing, and A. Kirillov, "Per-pixel classification is not all you need for semantic segmentation," *Advances in Neural Information Processing Systems*, vol. 34, pp. 17 864–17 875, 2021.
16. D.-P. Fan, G.-P. Ji, T. Zhou, G. Chen, H. Fu, J. Shen, and L. Shao, "Pranet: Parallel reverse attention network for polyp segmentation," in *International conference on medical image computing and computer-assisted intervention*. Springer, 2020, pp. 263–273.
17. J. Wang, Q. Huang, F. Tang, J. Meng, J. Su, and S. Song, "Stepwise feature fusion: Local guides global," in *International Conference on Medical Image Computing and Computer-Assisted Intervention*. Springer, 2022, pp. 110–120.
18. D. Jha, P. Smedsrud, M. Riegler, P. Halvorsen, T. Lange, D. Johansen, and H. Johansen, "Kvasir-seg: A segmented polyp dataset," *arXiv: Image and Video Processing, arXiv: Image and Video Processing*, Nov 2019.
19. J. Bernal, F. J. Sánchez, G. Fernández-Esparrach, D. Gil, C. Rodríguez, and F. Vilariño, "Wm-dova maps for accurate polyp highlighting in colonoscopy: Validation vs. saliency maps from physicians," *Computerized Medical Imaging and Graphics*, p. 99–111, Jul 2015. [Online]. Available: <http://dx.doi.org/10.1016/j.compmedimag.2015.02.007>
20. J. Bernal, J. Sánchez, and F. Vilariño, "Towards automatic polyp detection with a polyp appearance model," *Pattern Recognition*, p. 3166–3182, Sep 2012. [Online]. Available: <http://dx.doi.org/10.1016/j.patcog.2012.03.002>
21. J. Silva, A. Histace, O. Romain, X. Dray, and B. Granado, "Toward embedded detection of polyps in wce images for early diagnosis of colorectal cancer," *International Journal of Computer Assisted Radiology and Surgery*, p. 283–293, Mar 2014. [Online]. Available: <http://dx.doi.org/10.1007/s11548-013-0926-3>
22. N. Tajbakhsh, S. R. Gurudu, and J. Liang, "Automated polyp detection in colonoscopy videos using shape and context information," *IEEE transactions on medical imaging*, vol. 35, no. 2, pp. 630–644, 2015.
23. D. Vázquez, J. Bernal, F. J. Sánchez, G. Fernández-Esparrach, A. M. López, A. Romero, M. Drozdal, A. Courville *et al.*, "A benchmark for endoluminal scene segmentation of colonoscopy images," *Journal of healthcare engineering*, vol. 2017, 2017.
24. F. Tang, Z. Xu, Q. Huang, J. Wang, X. Hou, J. Su, and J. Liu, "Duat: Dual-aggregation transformer network for medical image segmentation," in *Chinese Conference on Pattern Recognition and Computer Vision (PRCV)*. Springer, 2023, pp. 343–356.

25. N. C. F. Codella, D. Gutman, M. E. Celebi, B. Helba, M. A. Marchetti, S. W. Dusza, A. Kalloo, K. Liopyris, N. Mishra, H. Kittler, and A. Halpern, "Skin lesion analysis toward melanoma detection: A challenge at the 2017 international symposium on biomedical imaging (isbi), hosted by the international skin imaging collaboration (isic)," in *2018 IEEE 15th International Symposium on Biomedical Imaging (ISBI 2018)*, Apr 2018. [Online]. Available: <http://dx.doi.org/10.1109/isbi.2018.8363547>
26. P. Tschandl, C. Rosendahl, and H. Kittler, "The ham10000 dataset, a large collection of multi-source dermatoscopic images of common pigmented skin lesions," *Scientific Data*, Aug 2018. [Online]. Available: <http://dx.doi.org/10.1038/sdata.2018.161>
27. X. Wang, X. Zhang, Y. Cao, W. Wang, C. Shen, and T. Huang, "Seggpt: Segmenting everything in context."
28. O. Ronneberger, P. Fischer, and T. Brox, "U-net: Convolutional networks for biomedical image segmentation," in *Medical Image Computing and Computer-Assisted Intervention—MICCAI 2015: 18th International Conference, Munich, Germany, October 5-9, 2015, Proceedings, Part III 18*. Springer, 2015, pp. 234–241.
29. J. Chen, Y. Lu, Q. Yu, X. Luo, E. Adeli, Y. Wang, L. Lu, A. L. Yuille, and Y. Zhou, "Transunet: Transformers make strong encoders for medical image segmentation," *arXiv preprint arXiv:2102.04306*, 2021.
30. D. Jha, P. H. Smedsrud, M. A. Riegler, D. Johansen, T. D. Lange, P. Halvorsen, and H. D. Johansen, "Resunet++: An advanced architecture for medical image segmentation," in *2019 IEEE International Symposium on Multimedia (ISM)*, Dec 2019. [Online]. Available: <http://dx.doi.org/10.1109/ism46123.2019.00049>